

# RF Central Solenoid Operation for Plasma Production and Current Drive in TST-2

Akira EJIRI, Yuichi TAKASE, Naoto TSUJII, Takahiro SHINYA, Satoru YAJIMA, Masateru SONEHARA, Hirokazu FURUI, Hiro TOGASHI, Hiroto HOMMA, Kenta NAKAMURA, Toshihiro TAKEUCHI, Yusuke YOSHIDA, Wataru TAKAHASHI, Kazuya TOIDA and Hibiki YAMAZAKI

*Graduate School of Frontier Sciences, The University of Tokyo, Kashiwa 277-8561, Japan*

(Received 16 September 2015 / Accepted 2 January 2016)

The RF central solenoid operation is a method for generating an inductive RF electric field in a device by which plasma can be produced and ohmically heated. Furthermore, it may drive the DC current via heating. Experiments were carried out in TST-2 to clarify this potential under a limited amount of flux swing ( $\pm 0.5$  mVs) of the central solenoid. It was found that it can produce plasma and drive the DC current up to approximately 0.6 kA on average when an external equilibrium field is applied. In addition, the DC current can be ramped up when the inductive RF field is applied to ECW power-sustained plasmas.

© 2016 The Japan Society of Plasma Science and Nuclear Fusion Research

Keywords: AC loop voltage operation, spherical tokamak, plasma production, current drive, flux swing

DOI: 10.1585/pfr.11.1202004

It is envisaged that steady-state tokamak reactors are equipped with no or a slim central solenoid (CS) [1]; thus, plasma production and plasma current  $I_p$  start-up in such situations are critical to fusion research. If we have a slim CS, we can apply an RF voltage and generate an inductive RF loop voltage  $V_{loop}$  within the limited flux swing. The inductive RF field would accelerate electrons and resultant electrons would be ohmically heated. Such an RF  $V_{loop}$  has been used as a heating tool in helical systems [2, 3]. On the contrary, several spherical tokamak (ST) experiments suggest that (DC) plasma currents can be started and sustained by a pressure-driven current [4–6], and there is a possibility of DC current driven by the RF  $V_{loop}$ . We report the results of the RF CS operation in TST-2 [7], where RF (a few kHz) voltage is applied to its CS (i.e., ohmic coil). It should be noted that the frequency in our experiment is much higher than that in the AC tokamak operation (e.g., [8, 9]), where the AC plasma current is intentionally adopted and issues related to cyclic discharges are studied.

TST-2 is a spherical tokamak device. When it is noninductively operated, typical plasmas have the following parameters: major radius  $R \sim 0.36$  m, minor radius  $a \sim 0.25$  m, toroidal magnetic field  $B_t < 0.3$  T, and plasma current  $I_p < 25$  kA. In typical ohmic-inductive discharges, the required flux swing of the CS is approximately 60 mVs to obtain  $I_p = 50$ –100 kA. To simulate a slim CS, the flux swing in the present experiments is  $\pm 0.5$  mVs.

To apply RF voltage to the CS, we built a power supply that comprises a DC capacitance (15.5 mF/500 V) and an H-bridge with eight insulated-gate bipolar transistors

(IGBTs) (Fig. 1). The H-bridge can switch the DC power supply connection with a frequency up to 10 kHz. The resultant  $V_{loop}$  exhibits a rectangular waveform, as shown in Fig. 2 (b), whereas the CS current has a triangular waveform owing to the inductance of the CS (Fig. 2 (a)). The switching is periodic, except that the initial cycle width is half of the succeeding cycles to suppress the DC flux component on average (see Fig. 2 (c)).

Figure 2 (d) shows equiflux surfaces at 9.7 ms, reconstructed using magnetic data (i.e., flux loops, pickup coils, saddle loops, and coil currents), calculated eddy currents, and parameterized eddy currents. The eddy currents are calculated by using a circuit model, wherein the vacuum vessel (V.V.) and other structures are represented by approximately 500 axisymmetric conductors (plus symbols in Fig. 2 (d)). Although the resistances of the conductors

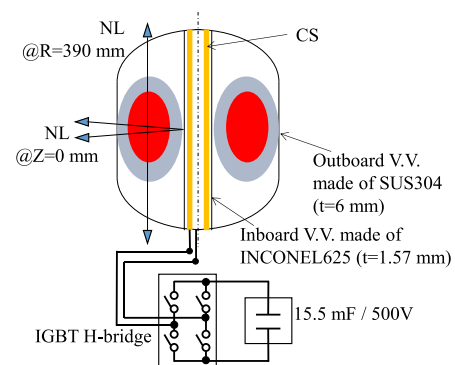


Fig. 1 Schematic of the AC loop voltage operation in TST-2.

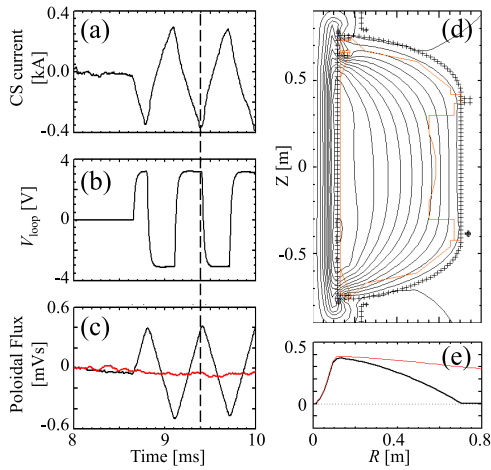


Fig. 2 Time evolutions of the CS current (a), inboard  $V_{loop}$  (b), inboard (black) and outboard (red) poloidal fluxes (c), contour plot of equiflux surfaces (d), and the midplane flux profile with eddy currents (black) and without eddy currents (red) (e) at 9.7 ms. The plus symbols in (d) represent the V.V. segments or other structures where eddy currents can flow.

are adjusted to reproduce certain experimental data, the accuracy of the circuit model worsens at short time scales. Therefore, we need to add the parameterized eddy currents to reproduce the magnetic data.

Although the inboard flux (black curve in Fig. 2 (c)) and inboard loop voltage (Fig. 2 (b)) roughly agree with those expected from the CS current, the outboard flux is nearly zero (red curve in Fig. 2 (c)). Thus, most of the CS flux is confined in the V.V. owing to its eddy current, as shown in Figs. 2 (d) and 2 (e). Note that the CS is located on the atmosphere side. Although the skin frequency of the inboard V.V. is quite high (about 130 kHz), the V.V. has overall long decay time constants (i.e., eigen values in the circuit model) of up to 5 ms. Therefore, the flux and  $V_{loop}$  decrease along the major radius, as shown in Fig. 2 (e). Note that the effect of eddy currents can be avoided when we operate the CS at a much lower frequency, such as 0.1 kHz. However, the flux swing increases with the inverse of frequency; such an operation is not preferred for the slim CS concept.

Several types of experiments were carried out. First, it was found that the RF CS operation can produce plasma when the vertical field is nearly zero and the filling gas pressure is sufficient, as shown in Figs. 3 (a) and 3 (b). In this case, about 7 ms after the RF  $V_{loop}$  ( $\pm 3.5$  V/1.6 kHz) was applied, plasma was produced, and positive and negative  $I_p$  are driven. Second, an external vertical field is applied just after the plasma production to simulate the RF wave power startup experiments in many STs. Then,  $I_p$  starts exhibiting an asymmetric AC waveform. The low-frequency component ( $< 1$  kHz) of  $I_p$  (red curve in Fig. 3 (a)) reached approximately 0.6 kA, and its direction

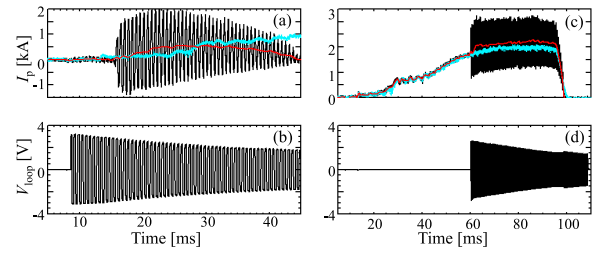


Fig. 3 Time evolutions of  $I_p$  (a) and (c), and the inboard  $V_{loop}$  (b) and (d). (a) and (b) show the case without ECW power, and (c) and (d) show the case where AC  $V_{loop}$  is applied to the target plasma sustained by ECW power. Light blue curves show the reference case where  $I_p$  is started and sustained by the ECW power only.

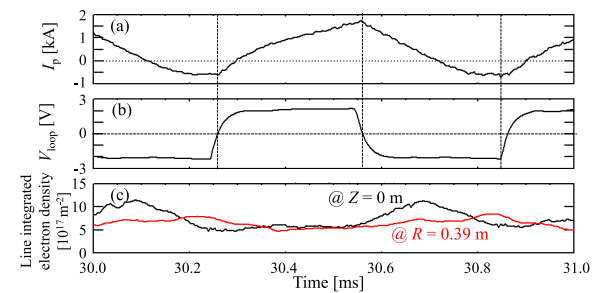


Fig. 4 Time evolution of  $I_p$  (a), the inboard  $V_{loop}$  (b) and the line integrated electron densities measured along two chords (shown in Fig. 1) (c).

with respect to the external vertical field is the direction that favors toroidal equilibrium. The flux swing in this discharge was  $\pm 0.5$  mVs, and the ratio of the flux swing to the driven current is similar to the ratios in standard ohmic discharges in TST-2. Third, the RF  $V_{loop}$  is superimposed on the ECW started up plasmas. The light blue curves in Fig. 3 show the waveforms of the reference ECW (3 kW) discharge without RF  $V_{loop}$ . During the flat top phase of  $I_p$ , an RF  $V_{loop}$  (2 kHz) is applied and  $I_p$  oscillates with amplitude  $\pm 1$  kA. As in the second case, the low-frequency component (red curve in Fig. 3 (c)) shows an increase in  $I_p$  by about 0.2 kA. Assuming that the effective  $V_{loop}$  is half of the inboard  $V_{loop}$  and that the power is resistively dissipated (i.e., ohmic heating), the power due to the RF  $V_{loop}$  becomes 0.5 kW, which may contribute to the increase in  $I_p$  through an increase in pressure.

Figure 4 shows the details of the discharge in Fig. 3 (a). When  $V_{loop}$  flips sign,  $I_p$  starts to change direction. The line-integrated densities are similar to those in the ECW-sustained discharges. Although visible CCD camera images show that the emission intensity is strongest on the inboard side, where the RF  $V_{loop}$  is strongest, the line-integrated electron density near the center of the V.V. is finite and does not disappear even when  $I_p$  becomes zero.

We discuss the applicability of the present scenario

to a reactor, considering the plasma initiation scenario in ITER [10], where the inboard side electric field  $E_T$  is 0.4 V/m, and 20 MW were consumed by the V.V. eddy current before the start of the plasma current. To date, the minimum inboard  $E_T$  for the plasma production was 1.6 V/m in TST-2, and  $E_T$  must be minimized to apply the present scenario to a superconducting CS and to decrease the power consumption owing to the eddy current. The RF frequency in our experiments was in the range of 1 - 10 kHz, whereas in ITER, the frequency must be lower than the inboard V.V. penetration frequency of 17 Hz. Furthermore, the frequency of the RF must be higher than the inverse of the energy confinement time to use the scenario as a heating tool. For the case of ITER-like initial plasma, the lower limit frequency is less than approximately 0.1 Hz, considering the neo-Alcator energy confinement scaling. If we adopt a normal conductor CS with a small flux swing, the

above requirements will be mitigated.

In summary, the RF CS operation with frequencies in the order of kHz was tested in TST-2, and it was found that the operation can produce plasma, drive the DC current, and ramp up the current.

- [1] K. Tobita *et al.*, Nucl. Fusion **47**, 892 (2007).
- [2] Y. Funato, S. Kitajima and H. Watanabe, Jpn. J. Appl. Phys. **23**, L779 (1984).
- [3] S. Kitajima *et al.*, J. Plasma Fusion Res. Ser. **1**, 219 (1998).
- [4] C.B. Forest *et al.*, Phys. Rev. Lett. **68**, 3559 (1992).
- [5] T. Yoshinaga *et al.*, J. Plasma Fusion Res. **81**, 333 (2005).
- [6] A. Ejiri *et al.*, Nucl. Fusion **46**, 709 (2006).
- [7] Y. Takase *et al.*, Nucl. Fusion **41**, 1543 (2001).
- [8] O. Mitarai *et al.*, Nucl. Fusion **32**, 1801 (1992).
- [9] O. Mitarai *et al.*, Nucl. Fusion **36**, 1335 (1996).
- [10] Y. Gribov *et al.*, Nucl. Fusion **47**, S385 (2007).